IEEE Access
Multidisciplinary | Rapid Review | Open Access Journal

Received August 30, 2020, accepted September 14, 2020, date of publication September 18, 2020,
date of current version September 30, 2020.

Digital Object Identifier 10.1109/ACCESS.2020.3024966

Evaluation of Hybrid Energy Storage Systems Using Wavelet and Stretched-Thread Methods

YAGO A. SANTOS, (Student Member, IEEE), MATHEUS P. M. NUNES, (Student Member, IEEE), LUCAS A. C. LEMES, (Student Member, IEEE), AND EDSON C. BORTONI, (Senior Member, IEEE)

Electric and Energy Systems Institute, Itajubá Federal University, Itajubá 37500-903, Brazil

Corresponding author: Edson C. Bortoni (bortoni@unifei.edu.br)

ABSTRACT This paper presents a methodology to evaluate hybrid energy storage systems in hybrid energy systems. While Wavelet is used to decompose the net load in temporal segments, the stretched-thread method is used to evaluate the influence of energy storage, instead of conventional optimization techniques, conferring a visual approach. Proper selection of energy storage technologies for each time frame, as long as several sizing of different energy storage technologies is evaluated as well. The use of different methods and their application in a hybrid system are the main contributions of this piece.

INDEX TERMS Energy storage, hybrid power systems, renewable power generation.

I. INTRODUCTION

The intermittence of renewable generation is a natural behavior. Regardless of whether the renewable power source is hydro, wind or solar, the input's availability will always vary if it depends on 'mother nature.'

What makes one source different from another is the variation time frame. For example, wind velocity can change in a short period. Despite solar irradiation being present from dawn until dusk peaking at noon, variations of irradiation on the soil level may be observed on a cloudy day. The same thing happens with hydropower. Although variation in the water flow may be slow, the river flow can vary from drought to flood.

For instance, Fig. 1 shows the net power evolution on a typical spring day in California; the steepest slope is in the morning, and in the evening, the slope can be seen with a total load rate of about 4 GW/h in both periods [1].

For now, the generation intermittence is not welcome in power systems. The Independent System Operator programming depends on a reliable forecast of the available power and load behavior. Connected equipment suffers due to power intermittency, resulting in reducing the average efficiency and duration of life [2], [3].

Intermittence of the renewable generation can be reduced with energy storage systems (ESS) in such a way that energy can be stored when there is a surplus and used when there is a deficit, in turn flattening the general power. There are several types of ESS with many distinguishing characteristics.

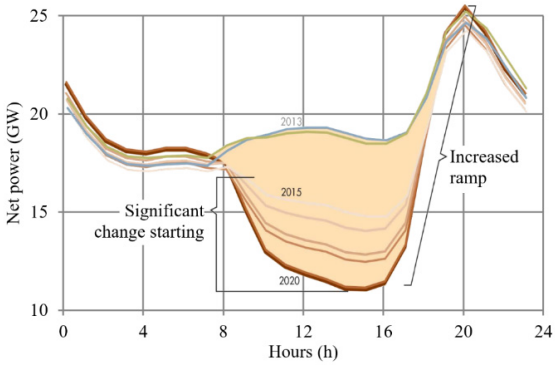

FIGURE 1. The "Duck curve," showing the net power variation in areas with high penetration of solar generation [1].

Fixed and variable costs, energy and power storage capacity, charging and discharging rates, gravimetric, volumetric, power and energy densities, maximum depth of discharge (DoD), lifetime in years and in cycles, self-discharging, roundtrip efficiency, technological maturity, among others, are listed as the main characteristics [4]–[6].

Several ESS can be seen in Fig. 2, relating their modular rated power with the stored energy for given time frames. This figure includes a superconducting magnetic coil (SMES), flow, thermal (TES), chemical (Li-ion) and molten salt batteries (NaS), compressed air (CAES), vanadium redox (VRB), pumped hydro (PHS), electrolysis fuel cell (H2), and synthetic methane (SNG) [7]–[9].

The associate editor coordinating the review of this manuscript and approving it for publication was Dusmanta Kumar Kumar Mohanta.

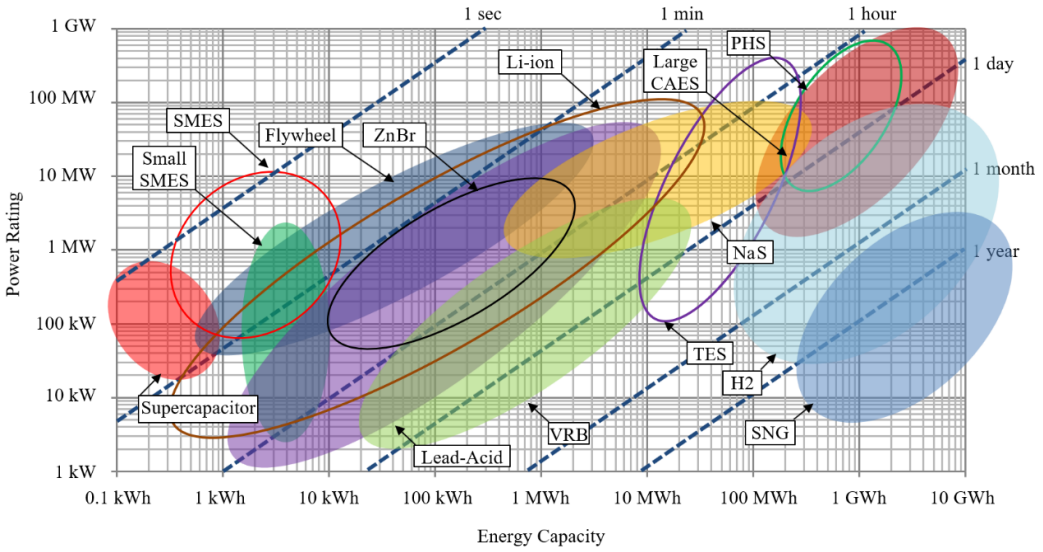

FIGURE 2. Energy storage technologies (adapted from [9]).

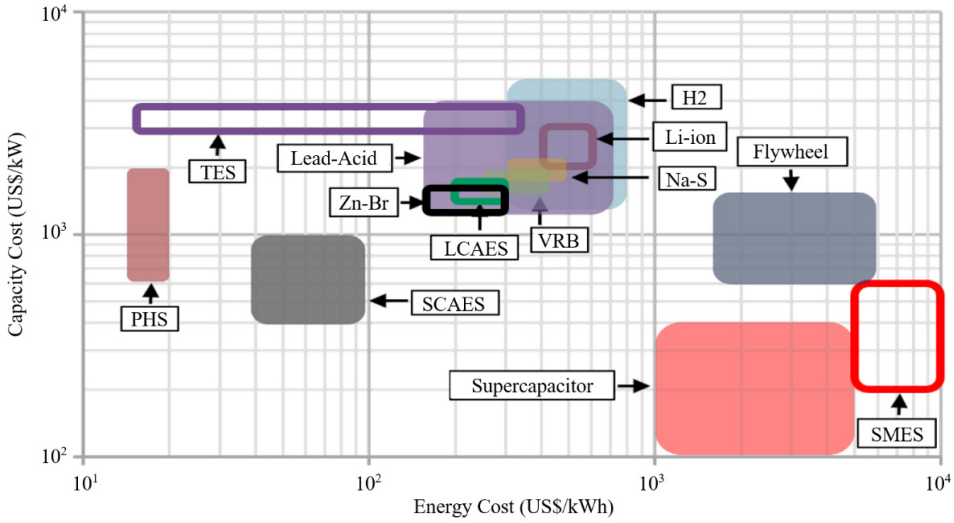

FIGURE 3. Cost characterization of several energy storage systems, presenting ranges of capacity and energy.

The costs associated to each technology are presented in Fig. 3.

It is recognized that only one type of ESS cannot handle the several time-frame variations of the components of a hybrid energy system. Therefore, EES's concept was evolved into the Hybrid Energy Storage System (HESS) defined by different types of EES hung together to cover all hybrid generation system requirements.

The analysis of HESS inclusion in the power systems has been extensively publicized [10], [11], and mainly deals with sizing and controlling the ESS system. In general, the sizing problem is solved with optimization techniques to minimize the acquisition and operating costs and improve grid health indexes [12]–[16]. Each ESS alternative's time scale is treated with filters [17]–[19], Fourier series, Wavelets, and neural networks [20]–[22].

However, most publications consider either solar or wind power generation covering a small number of BSS alternatives. On the other hand, this paper contributes by presenting a comprehensive methodology to decompose historical data in temporal segments of slow, average, fast, and very fast, making possible a convenient-sized ESS, according to Fig. 2, resulting in a HESS.

The slow power segment has annual coverage, the average segment covers a monthly period, the fast segment spans a week, and the very-fast segment covers a signal of daily variations. The inferior time limit of the intra-day evaluation depends on the minimum interval of time of available data.

The Conti-Varlet, along with the STM technique, is applied to define the HESS size to achieve hybrid power system full regularization [33]. Such a method is also used to evaluate the system's behavior when the HESS capacity is lower than that necessary for full regularization.

This method has been chosen because it is a very visual and intelligible technique.

Therefore, the joint use of both Wavelet and STM in evaluating HESS sizing was not found during an exhaustive literature review and comprised this paper's contribution.

Section II brings general information about the employed mathematical tools, section III presents the hybrid electrical system under study, section IV proceeds to the analysis of the hybrid power with temporal segmentation and, finally, section V presents the HESS evaluation considering different sizing and cost analysis, followed by the main conclusions of the research and bibliographical references.

II. MATHEMATICAL TOOLS

A. BRIEF WAVELET THEORY

Mathematical linear transforms are operations based on the inner product, orthogonality, and convolution, used to describe any function as a summation of infinite components of a base function. For instance, Fourier series uses sinusoids as a base function to describe any periodic signal, Gram-Charlier series uses the Gaussian probability density function as a base to describe any probability density function, and so forth.

Wavelet transform is not different as long as any function can be retrieved from a summation of any other wave-like function known as a mother wavelet (ψ), which may be Morlet, Meyer, Littlewood, or others. These functions have limited duration, null average, and nonzero norm. Therefore, a signal $f\,(t)$ can be reconstructed from the discrete wavelet transform [34], [35].

$$f(t) = \sum_{m}\sum_{n} \langle f, \psi_{m,n}\rangle \psi_{m,n}(t) \tag{1}$$

A dyadic discrete wavelet transform can be generated from a scaled and translated version of the mother function:

$$\psi_{m,n}(t) = 2^{-m/2}\psi\left(2^{-m}t - n\right) \tag{2}$$

where m and n are integer variables referring to the mother wavelet dilatation and shifting, allowing for an analysis of signals according to their scale. Short or large windowing is chosen for high- or low- frequency signals [35]. As in any transform, the inner product yields the base function's contents in the original signal:

$$\langle f, \psi_{m,n}\rangle = \int_{-\infty}^{+\infty} f\,(t)\,\psi_{m,n}\,(t)\,dt. \tag{3}$$

One of the most critical issues in using this mathematical tool is the definition of the right mother wavelet to be used. In this case, Meyer mother wavelet was chosen because of its sound time-frequency localization [36], [37].

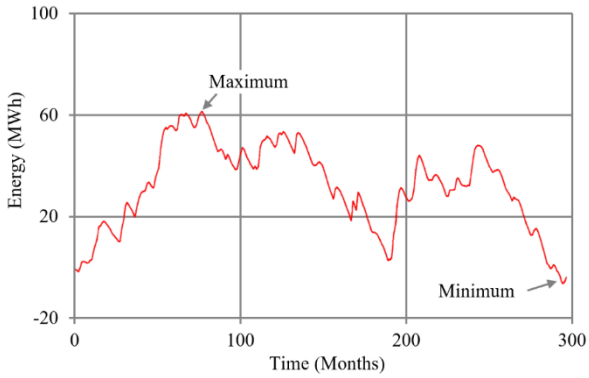

FIGURE 4. Differential Rippl diagram (adapted from [13]).

B. THE STRETCHED-THREAD METHOD

If power is integrated over time in a definite period, it will result in a curve of energy departing from zero and finishes at a given value. Nevertheless, if power minus average power is integrated over time, it will result in a curve of energy that departs from zero and ends in zero because, in the end, the integrated power over time is the average power itself. The obtained curve is the differential Rippl diagram, which has been used to define reservoirs volume for hydropower plants for long. An example of the Rippl diagram is shown in Fig. 4, already modified for the power storage case.

When the method was developed more than a hundred years ago, this diagram was used to be differential in volume, i.e., the volume created by inflows minus the average flow [38]. Translating the problem into electricity terms, now the resultant diagram is the differential energy, which is the instant power minus the average power, integrated over time. Mathematically it is:

$$E_{DIFF}(t) = \int P(t) - \bar{P}dt \tag{4}$$

The Conti-Varlet diagram is obtained when the storage capacity (E_{SC}) is added to the Differential Rippl diagram, defining an additional line, as shown in Fig. 5. The regularized power, i.e., the power that can be taken from the system considering the smoothing effect of the ESS, is obtained through the stretched-thread method (STM), i.e., the shortest path of optimization problem solution. Within the several methods available to solve this problem, a simple solution can be found in [38]. E_{ST} is the energy that can be exploited from the ESS. The power output may be obtained from the inverse of (4) applied to E_{ST}.

$$P\,(t) = \bar{P} + \frac{d}{dt}E_{ST}(t) \tag{5}$$

A constant power output, the long-term average power, can be identified when the derivative of the E_{ST} is zero. It is almost straightforward to infer that the necessary storage capacity will be the difference between the maximum and the minimum differential energy.

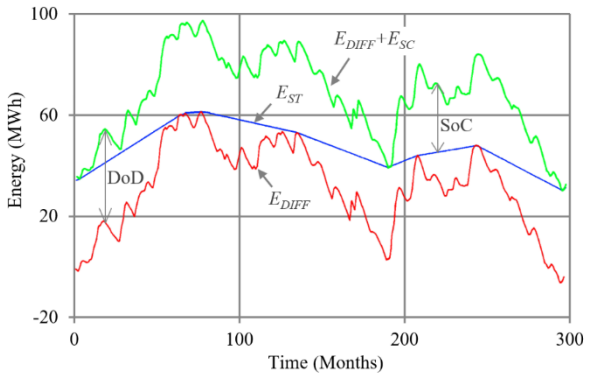

FIGURE 5. Conti-Varlet diagram and the STM (adapted from [13]).

Besides, in order to guarantee the same initial and final output powers, the slopes of E_{ST} in the beginning and in the end must be the same [39].

The STM does not define the size of the ESS, which would consider other variables that influence the acquisition decision of the ESS; instead, it evaluates the effects of ESS size in power smoothing. Therefore, the STM provides the optimal strategy for the continuous operation, the state of charge (SoC), navigating between the minimum and maximum storage capacity, i.e., the maximum DoD to keep the power as flat as possible. The upper limit constraint of the STM means that the battery is empty, and the lower limit constraint means that the battery is fully charged.

III. HYBRID ENERGY SYSTEM

A. SYSTEM CHARACTERIZATION

Hybrid systems are becoming very popular because the same landscape used for wind power generation can be used to install photovoltaic (PV) panels. Hybrid systems have also been applied in isolated areas to minimize the intermittence and increase the reliability of the renewable sources through to their parallel operation [40], [41].

The hybrid system studied in this paper is composed of wind and solar power generations, load, connection to the power system, and the energy storage system. The concept of the hybrid system is shown in Fig. 6.

The hybrid system accomplishes inverters connecting the solar and wind generation to the bus. The four ESS types are suitable for storing slow, average, fast, and very-fast power variations, as depicted in the electrical diagram of Fig. 7. An arrow pointing to the bus represents a positive flow; reversal flux is the opposite. Applying the Kirchhoff current law and rearranging, the net power required from the grid is:

$$P_S = P_L - P_W - P_{PV} \pm (\eta^*_{SS} P_{SS} + \eta^*_{SA} P_{SA} + \eta^*_{SF} P_{SF} + \eta^*_{SV} P_{SV}) \quad (6)$$

where P stands for power (MW), the subscripts denote power system (S), load (L), wind (W), solar (PV); SS, SA, SF, and SV, are slow, average, fast, and very-fast storage, along with the square-root of their roundtrip efficiency (η^*).

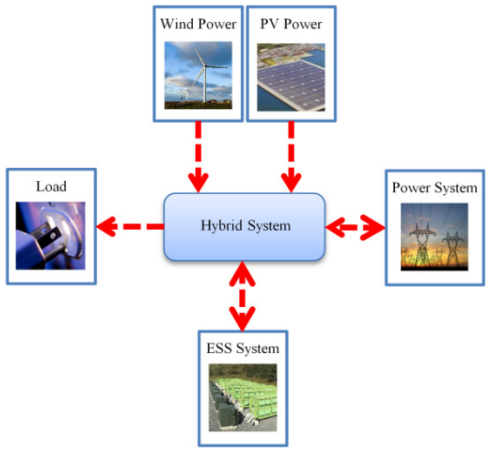

FIGURE 6. Hybrid system general concept.

The power supplied from the system is the summation of the renewable source power generation, minus the demanded power, following (6). Of course (6) considers the power supplied by the HESS components, which are equal to zero before calculation.

The ESS considered here performs the regularization of power during long periods, such as an entire year. This proposal is different from those systems used for daily power stabilization, taking advantage of available tariffs [42], [43]. Reactive power needs are not covered in this manuscript.

B. INPUT-OUTPUT CHARACTERIZATION

Information on solar global horizontal irradiance (GHI) and wind speed in this hybrid system were taken in intervals of ten minutes along a year, allowing for the determination of each renewable source's power generation, according to a specific directive. Load consumption was also integrated into intervals of ten minutes in order to obtain synchronized data. Figure 8 presents an excerpt of eight days from the available annual data of the load, wind speed, and solar GHI, obtained from [44].

All of these data were obtained for a specific location. Nevertheless, the proposed methodology is not dependent on the location and can be widely applied.

IV. NET POWER ANALYSIS

The renewable inputs were transformed into power generation, considering the efficiencies of the electronic power converters. Additionally, the net power in the main bus of the diagram from Fig. 7 was obtained. The net power was calculated according to (6). Even though the results were obtained for an entire year with intervals of ten minutes, the graph of Fig. 9 shows the results for eight days.

It can be observed that there are times of positive net power, which means that the local generation is smaller than the demand. Likewise, the hybrid system imports power from the system. On the other hand, there are times when the net power is negative, showing a power generation higher than the load and the hybrid system export power to the system.

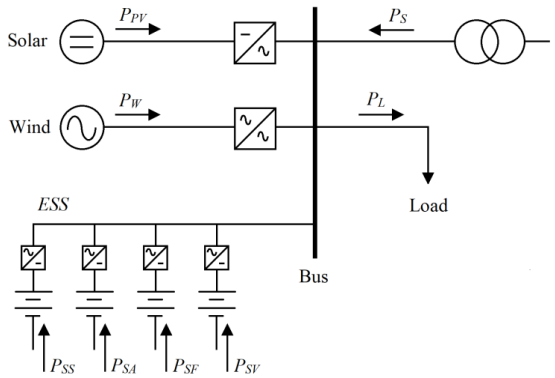

FIGURE 7. Hybrid system electrical diagram.

The average power is 4.14 MW, which means that in general, the hybrid system demand power from the system has a maximum demand of 13.93 MW and a maximum surplus of 9.78 MW.

Therefore, using the wavelet as mentioned earlier theory, it is possible to decompose the net power in signals of slow variation with annual coverage, the average variation that covers monthly periods, fast variations that spans a week, and very-fast signals for daily variations with an intra-hour resolution, in this case, sampled at 10-minute intervals.

While the yearly variation can be identified to size an ESS capable of storing high volumes of energy during an extended period, it is recognized that the variation in this time frame is minimal. The variations in this scale are plenty compatible with the variations in the bulk power system, which can easily be absorbed by just that. On the other hand, decomposition can be accomplished in smaller time frames, allowing for faster ESS sizing.

Figure 10 presents the results of annual net power decomposition for very fast, fast, average, and slow variations, whose summation is precisely the net power of the systems. As previously stated, the difference between the maximum and minimum differential Rippl diagram to these signals allows for knowing the capacities of each ESS necessary to guarantee flat operation. The results of the differential Rippl diagram application are shown in Fig. 11.

V. ESS SIZING EVALUATION

A. ESS FOR COMPLETE REGULARIZATION

With the tools and information presented in Sections II and III, respectively, the DoD necessary to achieve a flat net power (one may say total regularization) for each component of the ESS is obtained. Table 1 presents the energy capacities for the slow, average, fast, and very-fast HESS components. Notice that these values consider the maximum DoD. The energy storage capacities were obtained from the difference between the maximum and minimum of the results presented in Fig. 11, while the power storage capacity is the energy divided by the number of hours in the time frame, i.e., 8760 hours for a year, 720 hours for a month, 180 hours for a week, and 24 hours for a day. Of course, rated capacity and roundtrip efficiency depend on the chosen ESS.

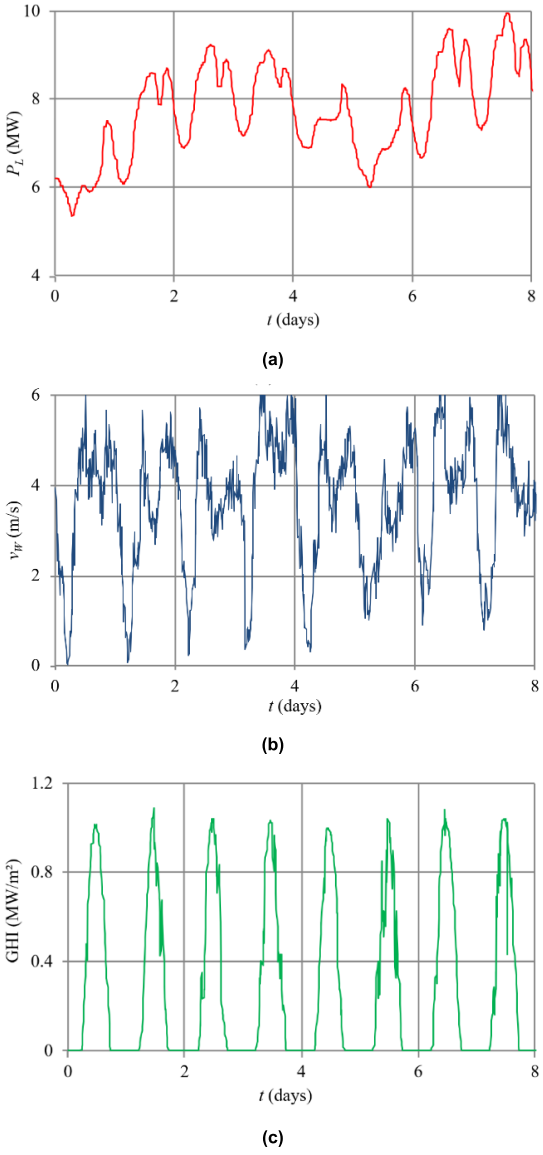

FIGURE 8. Hybrid energy system characterization considering load behavior (a), wind speed (b), and global horizontal irradiance (c).

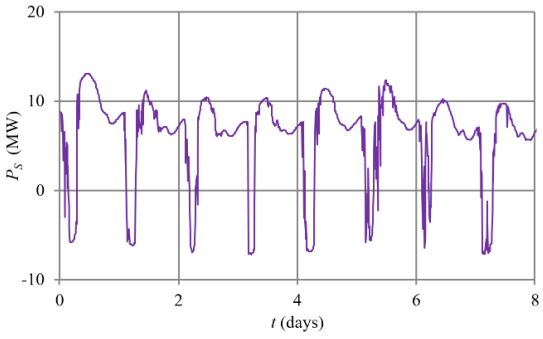

FIGURE 9. Hybrid energy system net power.

Figure 12 shows the influence of each component of the ESS in the behavior of the net power's temporal segments.

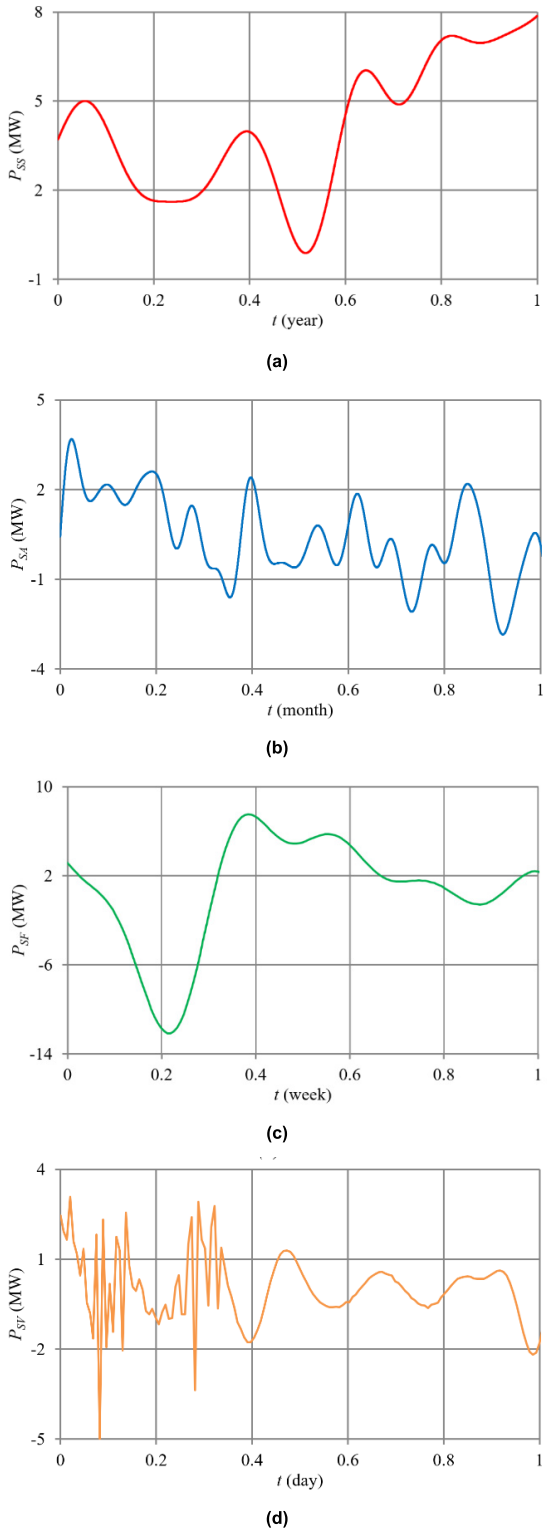

FIGURE 10. Decomposition of the net power in small (P_{SS}) average (P_{SA}), fast (P_{SF}), and very-fast (P_{SV}) variations regarding respectively for an entire year, month, week, and daily analysis with intra-hour demand variations.

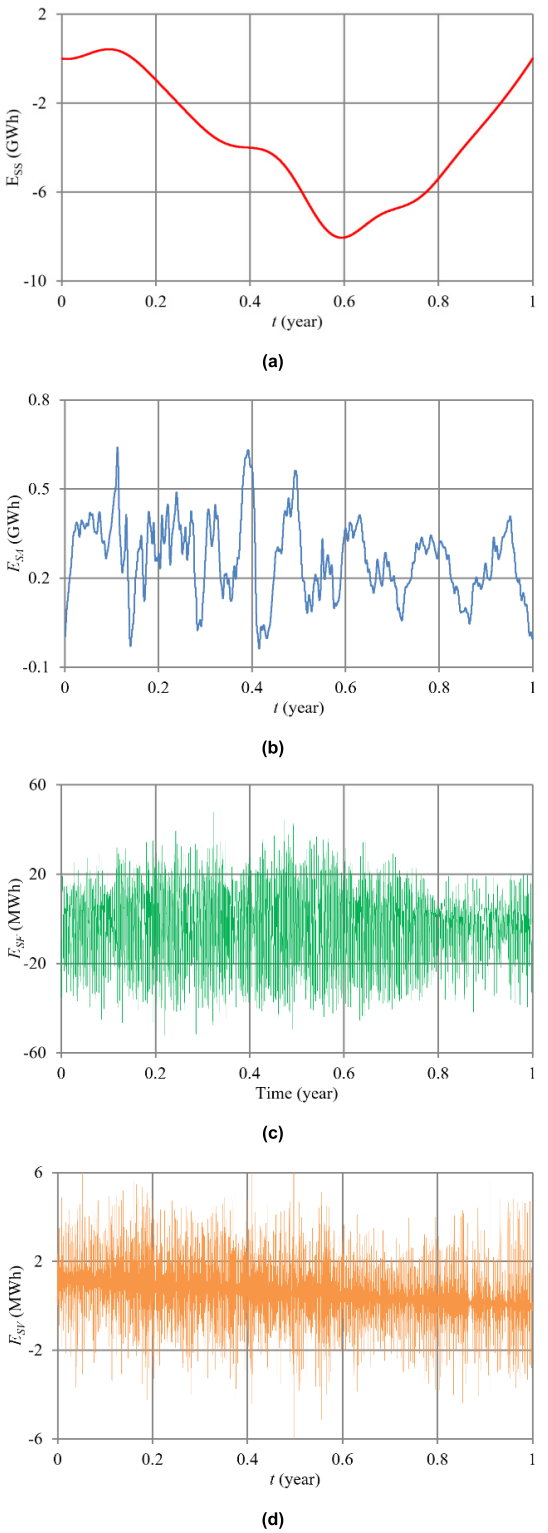

FIGURE 11. Differential Rippl diagrams for the load considering its small (E_{SS}), average (E_{SA}), fast (E_{SF}) and very-fast (E_{SV}) components.

The thin lines refer to original net power, without any ESS, while the thicker lines refer to the consequences of including different ESS in the hybrid power system. This evaluation is obtained by applying the STM. The integration of the original net power results in the inferior limit to the stretched-thread line, while the addition of the available storage capacity to this inferior limit leads to the upper limit. Therefore,

TABLE 1. Storage capacity of the HESS components.

Time frame	Storage Capacity (MWh)	Storage Capacity (kW)
Slow	8869.	1012.
Average	677.6	941.1
Fast	99.80	554.4
Very-fast	12.96	540.0

the energy that can be exploited from the EES, and its influence over the original net power is calculated.

Total regularization, resulting in flat net power, is obtained with the inclusion of full HESS capacity depicted in Table 1, and the outcome is shown in Fig. 12(a). The full regularization achieves the average demand of the system, i.e., 4.14 MW precisely. The regulation with the absence of long-term ESS, i.e., the EES necessary to cover the slow time frame, is presented in Fig. 12(b). The case in which the long-term and mid-term EES are unavailable; in other words, only fast and very-fast EES are present, is shown in Fig. 12(c).

Figure 12(d) shows the 30-day zooming of Fig.12(c), allowing watch the variation of the net power over the day. Although significant reduction of the undesired intermittence can be seen, variations can still be noticed. In Fig. 12(d), close to the 40-th day, for instance, the net power decreases from 9 MW to -6 MW in about 36 hours, resulting in a rate of roughly 0.4 MW/h. Therefore, the decision-maker can now evaluate the real need for any component of the HESS.

B. ESS FOR PARTIAL REGULARIZATION

The previous analysis studied the influence of exclusion of a HESS temporal component in the regularization of the total net power. In that case, it was considered full capacity for full regularization for each HESS component. Nevertheless, due to capital restrictions, a smaller capacity of HESS components may be acquired. Therefore, simulations were carried out to understand the effect of the size of each temporal component ESS in the resultant net power.

Figure 13 presents some of the results of this research, where Fig. 13(a) is related to the analysis of average time frame contents in the net power. Simulations considering 0%, 25%, and 50% of the necessary storage capacity for full regularization were simulated. The same results are presented in Fig. 13(b) and Fig. 13(c) for fast and very-fast time frames, respectively. In these cases, 0%, 50%, and 75% of the necessary storage capacity for full regularization in these time frames were simulated. It can be seen that 50% of the required ESS is enough to obtain suitable regularization.

In few words, the control and dispatching of the HESS is done by the continuous and adaptive forecasting of the electricity demand, solar and wind incidences, for the considered time frames, i.e., day, week, month, and year. Therefore, the operation and control of very-fast, fast, average, and slow ESS are rules of operation are defined.

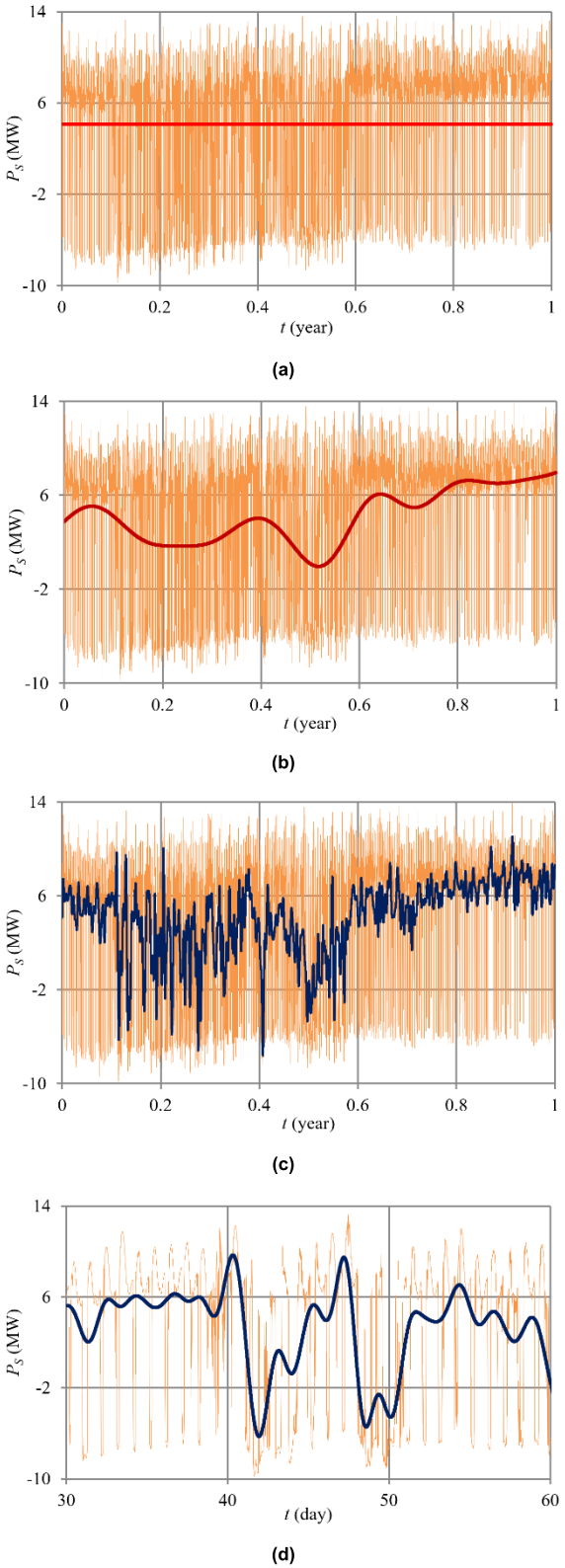

FIGURE 12. Evaluation of the convenience of using temporal components ESS in reducing undesirable intermittence.

C. COST EVALUATION

The selection of ESS includes the evaluation of several variables that defines the decision making. Many of the variables

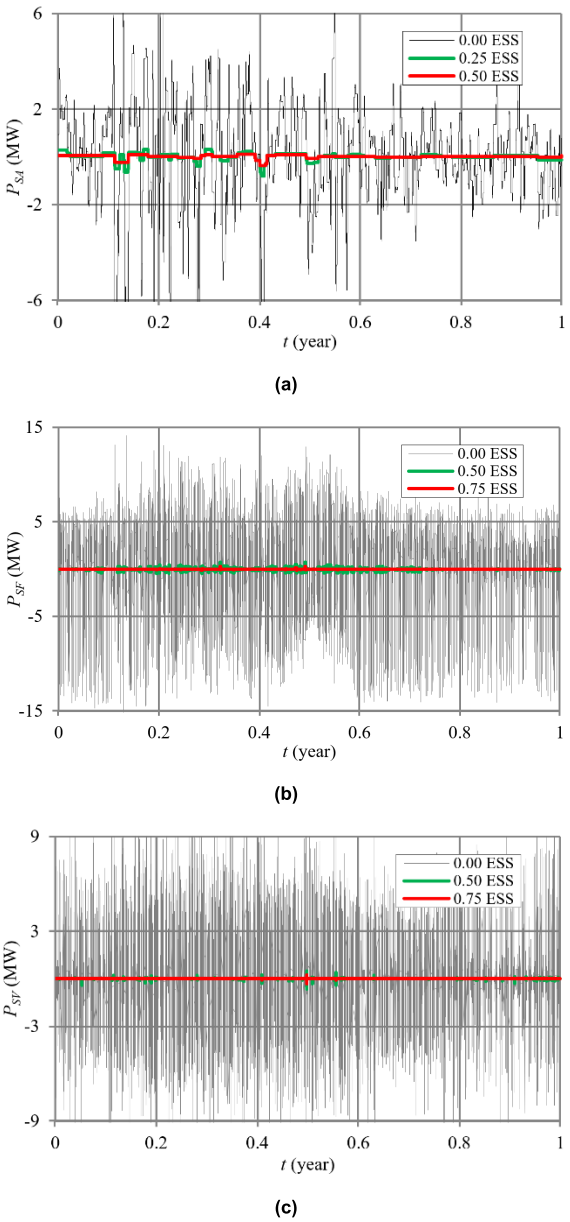

FIGURE 13. Evaluation of the influence of storage capacity alternatives in the regularization of the net power temporal components.

were mentioned in the introduction of this manuscript. No doubt, one of the most important selection criteria is the final cost. The estimation of the cost of ESS is based in Fig. 3, according to previous studies [45]–[49].

The analysis of Fig. 3 shows three definite clusters of energy costs. This information is the long-term cost that, in the end, it will have a preponderant weight over the capacity cost. In one group the energy cost varies from 10^1 to 10^2 US$/kWh while another group shows a variation from 10^2 to 10^3 US$/kWh, and finally, the third group with an energy cost between 10^3 and 10^4 US$/kWh.

That is the main benefit of the proposed method. When establishing four levels of temporal segments, and leaving the slow variation to be absorbed by the power system. It results that a more suitable HESS is chosen than a single ESS in order to cover the whole electric system requirement, as shown in Table 1, including the cost of the system.

VI. CONCLUSION

The intermittence associated with the renewable generation is long known and is not welcomed in the power system due to the flexibility challenges imposed on the Independent System Operator and equipment lifetime reduction, among other reasons. The use of ESS has become a suitable solution through storing energy when there is a surplus and releasing it when there is a deficit of power in the system, reducing the undesirable intermittence.

On the other hand, there are several ESS with different power ratings, energy, timing, and costs. The costs are directly proportional to the storage capacity and inversely proportional to its management time.

Therefore, this paper presented a wavelet-based strategy to divide the net power into components of slow, average, fast, and very-fast temporal segments, allowing for different ESS selection and application and resulting in a HESS.

The slow storage has an annual coverage with a monthly resolution; the average storage covers a monthly period with a weekly resolution, the fast storage spans a week with a daily resolution and the very-fast storage that evaluates intra-hour intervals throughout a day.

An old technique used to size reservoir in hydropower plants was recovered and modernized to use computational tools, was also applied to evaluate ESS. The net power of a hybrid system with PV and wind generations, load, connected to the grid, was decomposed in time frames, and the storage systems were appropriately studied.

The application showed that the power system could absorb slow and average variations, but fast and very-fast variations are subject to energy storage design and dispatch. The use of the proposed net-load decomposition is exciting and brings economic benefits as the higher storage capacities are left to slow and average ESS, and the smaller storage capacities are granted to fast and very-fast EES.

In the same way, variations of the storage capacity in those time frame components were applied. The simulations showed that even more economic benefits could be obtained if storages lower than necessary to full regularization is used.

The development of a suitable control system to conveniently manage the ESS may control the dispatch of the HESS components is subject to future works.

ACKNOWLEDGMENT

The authors would like to thank FAPEMIG, INERGE, CAPES, and CNPq for their continued support in conducting research.

REFERENCES

[1] P. Denholm, M. O'Connell, G. Brinkman, and J. Jorgenson, "Overgeneration from solar energy in California: A field guide to the duck chart," NREL, Golden, CO, USA, Tech. Rep. NREL/TP-6A20-65023, 2015.

[2] E. C. Bortoni, M. K. I. Uemori, B. T. Araujo, J. V. Bernardes, Jr., J. J. Rocha E., and R. T. Siniscalchi, "Accurate methodology to obtain efficiency mapping of synchronous machines," in *Proc. IEEE Power Energy Soc. Gen. Meeting, Virtual Conf.*, Aug. 2020.
[3] W. Yang, P. Norrlund, L. Saarinen, A. Witt, B. Smith, J. Yang, and U. Lundin, "Burden on hydropower units for short-term balancing of renewable power systems," *Nature Commun.*, vol. 9, no. 1, p. 2633, Dec. 2018.
[4] H. L. Ferreira, R. Garde, G. Fulli, W. Kling, and J. P. Lopes, "Characterization of electrical energy storage technologies," *Energy*, vol. 53, pp. 288–298, May 2013.
[5] B. F. Nunes, Y. F. F. C. Silva, and E. C. Bortoni, "Optimized selection and operation of electrical energy storage systems," in *Proc. IEEE Power Energy Soc. Gen. Meeting*, Jul. 2015, pp. 1–5.
[6] E. M. G. Rodrigues, R. Godina, S. F. Santos, A. W. Bizuayehu, J. Contreras, and J. P. S. Catalão, "Energy storage systems supporting increased penetration of renewables in islanded systems," *Energy*, vol. 75, pp. 265–280, Oct. 2014.
[7] *Electricity Storage Handbook in Collaboration With*, document US DOE/EPRI, NRECA, Albuquerque, NM, USA, 2015.
[8] *International Electrotechnical Commission (IEC)*, Electrical Energy Storage, White Paper White Paper, Geneva, Switzerland, 2011.
[9] X. Luo, J. Wang, M. Dooner, and J. Clarke, "Overview of current development in electrical energy storage technologies and the application potential in power system operation," *Appl. Energy*, vol. 137, pp. 511–536, Jan. 2015.
[10] S. Hajiaghasi, A. Salemnia, and M. Hamzeh, "Hybrid energy storage system for microgrids applications: A review," *J. Energy Storage*, vol. 21, pp. 543–570, Feb. 2019.
[11] A. A. Khodadoost Arani, G. B. Gharehpetian, and M. Abedi, "Review on energy storage systems control methods in microgrids," *Int. J. Electr. Power Energy Syst.*, vol. 107, pp. 745–757, May 2019.
[12] Y. Jiang, L. Kang, and Y. Liu, "A unified model to optimize configuration of battery energy storage systems with multiple types of batteries," *Energy*, vol. 176, pp. 552–560, Jun. 2019.
[13] K. Hesaroor and D. Das, "Optimal sizing of energy storage system in islanded microgrid using incremental cost approach," *J. Energy Storage*, vol. 24, Aug. 2019, Art. no. 100768.
[14] H. Xie, X. Teng, Y. Xu, and Y. Wang, "Optimal energy storage sizing for networked microgrids considering reliability and resilience," *IEEE Access*, vol. 7, pp. 86336–86348, 2019.
[15] N. K. Paliwal, A. K. Singh, N. K. Singh, and P. Kumar, "Optimal sizing and operation of battery storage for economic operation of hybrid power system using artificial bee colony algorithm," *Int. Trans. Electr. Energy Syst.*, vol. 29, no. 1, p. e2685, Jan. 2019.
[16] Y. Liu, Y. Zhu, W. Xu, J. Gou, Y. Xiang, and J. Liu, "Dynamic wavelet decomposition based multi-objective operation model for HESS enabling wind power output smoothing," *Energy Procedia*, vol. 142, pp. 1462–1467, Dec. 2017.
[17] H. Liu, D. Li, Y. Liu, M. Dong, X. Liu, and H. Zhang, "Sizing hybrid energy storage systems for distributed power systems under multi-time scales," *Appl. Sci.*, vol. 8, no. 9, p. 1453, Aug. 2018.
[18] Y. Sun, X. Tang, X. Sun, D. Jia, Z. Cao, J. Pan, and B. Xu, "Model predictive control and improved low-pass filtering strategies based on wind power fluctuation mitigation," *J. Modern Power Syst. Clean Energy*, vol. 7, no. 3, pp. 512–524, May 2019.
[19] Z. Yan and X.-P. Zhang, "General energy filters for power smoothing, tracking and processing using energy storage," *IEEE Access*, vol. 5, pp. 19373–19382, 2017.
[20] I. N. Moghaddam and B. Chowdhury, "Optimal sizing of hybrid energy storage systems to mitigate wind power fluctuations," in *Proc. IEEE Power Energy Soc. Gen. Meeting (PESGM)*, Jul. 2016, pp. 1–5.
[21] S. Majumder, S. A. Khaparde, A. P. Agalgaonkar, P. Ciufo, S. Perera, and S. V. Kulkarni, "DFT-based sizing of battery storage devices to determine day-ahead minimum variability injection dispatch with renewable energy resources," *IEEE Trans. Smart Grid*, vol. 10, no. 1, pp. 626–638, Jan. 2019.
[22] H. Shao, H. Wei, X. Deng, and S. Xing, "Short-term wind speed forecasting using wavelet transformation and AdaBoosting neural networks in yunnan wind farm," *IET Renew. Power Gener.*, vol. 11, no. 4, pp. 374–381, Mar. 2017.
[23] X. Li and S. Wang, "A review on energy management, operation control and application methods for grid battery energy storage systems," *CSEE J. Power Energy Syst.*, early access, 2019, pp. 1–15.
[24] F. Conte, F. D'Agostino, P. Pongiglione, M. Saviozzi, and F. Silvestro, "Mixed-integer algorithm for optimal dispatch of integrated PV-storage systems," *IEEE Trans. Ind. Appl.*, vol. 55, no. 1, pp. 238–247, Jan./Feb. 2010.
[25] H. Zhao and W. Guo, "Hierarchical distributed coordinated control strategy for hybrid energy storage array system," *IEEE Access*, vol. 7, pp. 2364–2375, 2019.
[26] X. Zhang, J. Gu, L. Hua, and K. Ma, "Enhancing performances on wind power fluctuation mitigation by optimizing operation schedule of battery energy storage systems with considerations of operation cost," *IEEE Access*, vol. 7, pp. 94072–94083, 2019.
[27] B. Li, X. Mo, and B. Chen, "Direct control strategy of real-time tracking power generation plan for wind power and battery energy storage combined system," *IEEE Access*, vol. 7, pp. 147169–147178, 2019.
[28] F. Zhang, Z. Hu, K. Meng, L. Ding, and Z. Y. Dong, "Sequence control strategy for hybrid energy storage system for wind smoothing," *IET Gener., Transmiss. Distrib.*, vol. 13, no. 19, pp. 4482–4490, Oct. 2019.
[29] T. Trung, S.-J. Ahn, J.-H. Choi, S.-I. Go, and S.-R. Nam, "Real-time wavelet-based coordinated control of hybrid energy storage systems for denoising and flattening wind power output," *Energies*, vol. 7, no. 10, pp. 6620–6644, Oct. 2014.
[30] Q. Jiang and H. Hong, "Wavelet-based capacity configuration and coordinated control of hybrid energy storage system for smoothing out wind power fluctuations," *IEEE Trans. Power Syst.*, vol. 28, no. 2, pp. 1363–1372, May 2013.
[31] T. Guo, Y. Liu, J. Zhao, Y. Zhu, and J. Liu, "A dynamic wavelet-based robust wind power smoothing approach using hybrid energy storage system," *Int. J. Electr. Power Energy Syst.*, vol. 116, Mar. 2020, Art. no. 105579.
[32] A. Atif and M. Khalid, "Saviztky–Golay filtering for solar power smoothing and ramp rate reduction based on controlled battery energy storage," *IEEE Access*, vol. 8, pp. 33806–33817, 2020.
[33] V. Kleměs, "One hundred years of applied storage reservoir theory," *Water Resour. Manage.*, vol. 1, no. 3, pp. 159–175, Sep. 1987.
[34] Z. He, *Wavelet Analysis and Transient Signal Processing Applications for Power Systems*, 1st ed. Singapore: Wiley, 2016.
[35] L. Debnath, F. A. Shah, *Lecture Notes on Wavelet Transforms. Compact Textbooks in Mathematics*. Basel, Switzerland: Birkhäuser, 2017.
[36] M. O. Oliveira, J. H. Reversat, and L. A. Reynoso, *Wavelet Transform Analysis to Applications in Electric Power Systems*. London, U.K.: IntechOpen, 2019.
[37] J. Frunt, W. L. Kling, and P. F. Ribeiro, "Wavelet decomposition for power balancing analysis," *IEEE Trans. Power Del.*, vol. 26, no. 3, pp. 1608–1614, Jul. 2011.
[38] V. Kleměs, "Storage-mass-curve analysis in a systems-analytic perspective," *Water Resour. Res.*, vol. 15, no. 2, p. 12, Apr. 1979.
[39] P. A. V. Vieira, E. C. Bortoni, and A. S. Bretas, "A new approach of contivarlet method applied to a PV system to size a battery energy storage," in *Proc. IEEE Milan PowerTech*, Jun. 2019, pp. 1–5.
[40] J. J. Roberts, A. M. Cassula, J. L. Silveira, E. da Costa Bortoni, and A. Z. Mendiburu, "Robust multi-objective optimization of a renewable based hybrid power system," *Appl. Energy*, vol. 223, pp. 52–68, Aug. 2018.
[41] S. Sinha and S. S. Chandel, "Review of recent trends in optimization techniques for solar photovoltaic–wind based hybrid energy systems," *Renew. Sustain. Energy Rev.*, vol. 50, pp. 755–769, Oct. 2015.
[42] D. Meneghel, E. D. C. Bortoni, and A. Karimi, "Boosting DC/AC ratio of PV plant for BESS integration on DC side," in *Proc. IEEE Conf. Technol. Sustainability (SusTech)*, Nov. 2018, pp. 1–4.
[43] N. Müller, S. Kouro, P. Zanchetta, P. Wheeler, G. Bittner, and F. Girardi, "Energy storage sizing strategy for grid-tied PV plants under power clipping limitations," *Energies*, vol. 12, no. 9, p. 1812, May 2019.
[44] ONS. *Sub-Module 2.7—Minimal Requirements for Supervision, Control and Operation (in Portuguese)*. Accessed: Sep. 1, 2019. [Online]. Available: https://www.ons.org.br
[45] *Levelized Cost of Storage Analysis—Version 3.0*, Lazard, Hamilton, Bermuda. Nov. 2017.
[46] *Electricity Storage and Renewables: Costs and Markets to 2030*, International Renewable Energy AgencyIrena, Abu Dhabi, United Arab Emirates, 2017.
[47] B. Zakeri and S. Syri, "Electrical energy storage systems: A comparative life cycle cost analysis," *Renew. Sustain. Energy Rev.*, vol. 42, pp. 569–596, Feb. 2015.

[48] V. Jülch, "Comparison of electricity storage options using levelized cost of storage (LCOS) method," *Appl. Energy*, vol. 183, pp. 1594–1606, Dec. 2016.
[49] M. C. Argyrou, P. Christodoulides, and S. A. Kalogirou, "Energy storage for electricity generation and related processes: Technologies appraisal and grid scale applications," *Renew. Sustain. Energy Rev.*, vol. 94, pp. 804–821, Oct. 2018.

YAGO A. SANTOS (Student Member, IEEE) was born in Passa Quatro, Brazil, in January 1996. He is currently pursuing the bachelor's degree in electrical engineering and the master's degree with the Federal University of Itajubá (UNIFEI), Itajubá, Brazil. Since 2017, he has been a member of the Power Electronics and Industrial Control Group (GEPCI) in which he developed his first research project on active filters, signal processing and control. He is also a Researcher with the EXCEN, the Excellence Center in Energy Efficiency. His research interests include power electronics, power system analysis, renewable energy sources, electrical machines, distributed generation, and signal processing and control. He is a Student Member of the IEEE Power & Energy Society.

MATHEUS P. M. NUNES (Student Member, IEEE) was born in Cruzília, Brazil, in June 1997. He is currently pursuing the bachelor's degree in electrical engineering with the Federal University of Itajubá (UNIFEI), Itajubá, Brazil. He is an Intern with the Electrical System Expansion Planning Department, CPFL Energy, Campinas, Brazil. He is also a Researcher with the EXCEN, the Excellence Center in Energy Efficiency. His research interests include smart grids, virtual power plants, renewable energy sources, distributed generation, and electrical machines. He is a Student Member of the IEEE Power & Energy Society and the Power Electronics Society.

LUCAS A. C. LEMES (Student Member, IEEE) was born in Piranguinho, Brazil, in December 1995. He is currently pursuing the bachelor's degree in electrical engineering with the Federal University of Itajubá (UNIFEI). He has worked as a Researcher with the EXCEN, the Excellence Center in Energy Efficiency. He is also an Intern with INATEL, Santa Rita do Sapucaí, Brazil, where he looks for electrical solutions for the implantation of mobile phone sites. His research interest includes statistical characterization of renewable inputs.

EDSON C. BORTONI (Senior Member, IEEE) was born in Maringá, Brazil, in 1966. He received the bachelor's degree in electrical engineering from the Federal University of Itajubá (UNIFEI), Itajubá, Brazil, in 1990, the M.Sc. degree in energy systems planning from the University of Campinas, Campinas, Brazil, in 1993, the D.Sc. degree in power systems from the Polytechnic School, University of São Paulo (USP), São Paulo, Brazil in 1998, and the Habilitation degree from USP, in 2012. He was a Professor with São Paulo State University, Guaratinguetá, Brazil. He was a Visiting Scholar with Montanuniversität Leoben, Austria, the École Polytechnique Fédérale de Lausanne, Switzerland, and the Politecnico di Torino, Italy. He is currently a Full Professor with UNIFEI. He is the Head of the EXCEN, the Excellence Center in Energy Efficiency. His research interests include electrical machine design, testing, and modeling, power generation, energy systems, sensors, and smart grids. He is a member of the EMC, WG-7 (IEEE STD. 115), WG-8 (IEEE STD. C50.13), WG-10 (IEEE STD. 1110), of the EMC Grid Code Task Force. He is a Fellow Member of the International Hydropower Association and the International Society of Automation. He is the Chair of the Generator Subcommittee and the WG-4 (IEEE STD. C50.12), and several technical sessions in important conferences, including PowerTech, the IEEE PES General Meeting, IEMDC, and others. He is the President of the Brazilian Energy Planning Society. He is an Assistant Editor and a Subject Editor of the *IET GTD Journal* and an Assistant Editor of *Flow Measurement and Instrumentation Journal*. He is a Distinguished Lecturer of the PES IEEE.